ANL-08/12

Argonne NATIONAL LABORATORY

Hydrogen Production by Water Dissociation Using Ceramic Membranes Annual Report for FY 2007

Energy Systems Division

About Argonne National Laboratory

Argonne is a U.S. Department of Energy laboratory managed by UChicago Argonne, LLC under contract DE-AC02-06CH11357. The Laboratory's main facility is outside Chicago, at 9700 South Cass Avenue, Argonne, Illinois 60439. For information about Argonne, see www.anl.gov.

Availability of This Report

This report is available, at no cost, at http://www.osti.gov/bridge. It is also available on paper to the U.S. Department of Energy and its contractors, for a processing fee, from:

U.S. Department of Energy
Office of Scientific and Technical Information
P.O. Box 62
Oak Ridge, TN 37831-0062
phone (865) 576-8401
fax (865) 576-5728
reports@adonis.osti.gov

ANL-08/12

Hydrogen Production by Water Dissociation Using Ceramic Membranes Annual Report for FY 2007

by
U. (Balu) Balachandran
Energy Systems Division, Argonne National Laboratory

contributors
L. Chen, S.E. Dorris, J.E. Emerson, T.H. Lee,
C.Y. Park, J.J. Picciolo, and S.J. Song

work supported by
U.S. Department of Energy
Office of Fossil Energy, National Energy Technology Laboratory

January 31, 2008

Contents

Figures

HYDROGEN PRODUCTION BY WATER DISSOCIATION USING CERAMIC MEMBRANES

ANNUAL REPORT FOR FY 2007

ARGONNE NATIONAL LABORATORY

Project Title: Hydrogen Production by Water Dissociation using Ceramic Membranes

NETL Project Manager: Richard Dunst

ANL Project PI: U. (Balu) Balachandran

B&R Code/Contract Number: AA-10-40-00-00-0/FWP 49347

Report Date: January 31, 2008

I. OBJECTIVE

The objective of this project is to develop dense ceramic membranes that, without using an external power supply or circuitry, can produce hydrogen via coal/coal gas-assisted water dissociation.

II. HIGHLIGHTS

1. Three types of material show promise as oxygen transport membranes (OTMs) that enable hydrogen to be produced via water splitting. They are Gd-doped CeO_2 (CGO)/Ni ceramic/metal composite, $SrFeCo_{0.5}O_x$ (SFC2), and Sr-Fe-Ti oxide (SFT).

2. Improvements in the sintering process and coating with porous surface layers gave a record-high rate for hydrogen production with Argonne OTMs. An SFC2 thin (<50 μm) film coated with porous SFC2 layers achieved a hydrogen production rate of ≈13 $cm^3/min\text{-}cm^2$.

3. The hydrogen production rate of CGO/Ni membranes was increased by coating them with porous layers and by making their microstructure finer.

4. Unlike SFC2 membranes, SFT membranes do not exhibit a sharp decrease in their hydrogen production rate as temperature falls below ≈825°C.

5. Methods have been developed for fabricating and testing OTM tubes. SFC2 tubes have been fabricated and are being tested.

III. INTRODUCTION

This project grew out of an effort to develop a dense ceramic membrane for separating hydrogen from gas mixtures such as those generated during coal gasification, methane partial oxidation, and water-gas shift reactions [1]. That effort led to the development of various cermet (i.e., ceramic/metal composite) membranes that enable hydrogen to be produced by two methods. In one method, a hydrogen transport membrane (HTM) selectively removes hydrogen from a gas mixture by transporting it through either a mixed protonic/electronic conductor or a hydrogen transport metal. In the other method, an oxygen transport membrane (OTM) generates hydrogen mixed with steam by removing oxygen that is generated through water splitting [1, 2].

This project focuses on the development of OTMs that efficiently produce hydrogen via the dissociation of water. Supercritical boilers offer very high-pressure steam that can be decomposed to provide pure hydrogen by means of OTMs. Oxygen resulting from the dissociation of steam can be used for coal gasification, enriched combustion, or synthesis gas production. Hydrogen and sequestration-ready CO_2 can be produced from coal and steam by using the membrane being developed in this project. Although hydrogen can also be generated by high-temperature steam electrolysis, producing hydrogen by water splitting with a mixed-conducting membrane requires no electric power or electrical circuitry.

Water dissociates into oxygen and hydrogen at high temperatures by the reaction:

$$H_2O(g) \Leftrightarrow H_2 + \frac{1}{2}O_2,$$

However, very low concentrations of hydrogen and oxygen are generated even at relatively high temperatures (e.g., 0.1 and 0.042% for hydrogen and oxygen, respectively, at 1600°C), because the equilibrium constant for the reaction is small [3]. This shortcoming can be overcome, at moderate temperatures, by using a mixed-conducting (electron- and ion-conducting) membrane to remove either oxygen or hydrogen, which shifts the equilibrium toward dissociation. If an OTM is used to produce hydrogen, the hydrogen production rate depends directly on the rate at which oxygen is removed from the water dissociation zone. The oxygen removal rate depends on the membrane's oxygen permeability (a function of the membrane's electron and oxygen-ion conductivities), the surface oxygen exchange kinetics, and the oxygen partial pressure (pO_2) gradient across the membrane [4-7]. To obtain a high hydrogen production rate, membranes should exhibit high electron and oxygen-ion conductivities, should possess good surface exchange properties, and should be exposed to a high pO_2 gradient.

Others have used mixed oxygen-ion/electron-conducting membranes to produce hydrogen by water dissociation, but the hydrogen production rate was modest even at high temperature (e.g., 0.6 cm^3 (STP)/min-cm^2 at 1683°C [8]) mainly because the membranes had low electronic conductivity. Using an OTM composed of an oxygen-ion conductor (CGO) and an electronic conductor (Ni), we achieved a significantly higher hydrogen production rate.

This rate increased with increases in temperature, water partial pressure on the hydrogen-production side of the membrane, and oxygen chemical potential gradient across the membrane. It also increased with decreasing membrane thickness, but surface reaction kinetics began to limit the hydrogen production rate for thin (< ≈0.5 mm) OTMs.

To be practical for hydrogen production, OTMs must give high hydrogen production rates and be available in a shape with a large active area, e.g., tubes. This report summarizes progress during FY 2007 toward the fabrication of practical OTMs. To increase the hydrogen production rate of CGO/Ni OTMs, we enhanced the surface reaction kinetics by increasing the area of the triple-phase boundary (i.e., the region where ionic conductor, electronic conductor, and gas phase meet). This was done by coating the membranes with porous layers and by producing the membranes with finer microstructures. We showed that other OTM compositions, $SrFeCo_{0.5}O_x$ (SFC2) and Sr-Fe-Ti-oxide (SFT), give promising hydrogen production rates due to their intrinsically favorable oxygen permeation rates. Without any microstructural modifications, SFC2 gives high hydrogen production rates, but limitations from surface reaction kinetics appear important even for relatively thick (≈1 mm) membranes. Adding porous layers to an ≈50-μm-thick SFC2 membrane gave a hydrogen production rate of ≈13 $cm^3/min\text{-}cm^2$, the highest hydrogen production rate yet obtained at Argonne. In addition to these efforts to increase the hydrogen production rate, we began developing methods for fabricating tubular OTMs.

IV. RESULTS

A) Gd-doped CeO_2 (CGO)/Ni Composite Membranes

Powder mixtures for CGO/Ni membranes were prepared by either reducing a CGO/NiO mixture (Praxair) in 4% H_2/balance He at 700°C for 10 h or by mechanically mixing CGO powder from Praxair Surface Technologies Specialty Ceramics with Ni powder (avg. particle size ≈3 μm). Disk-shape membranes were prepared by uniaxially pressing CGO/Ni powder and then sintering in 200 ppm H_2/balance N_2. Membranes made from mechanically mixed CGO/Ni powder were sintered at 1400°C for 10 h and had relatively coarse microstructures, whereas membranes made from CGO/NiO powder were sintered at 1150°C and had considerably finer microstructures. Only Ni and CGO were detected by X-ray diffraction analysis after sintering.

To measure the hydrogen production rate, both sides of a sintered disk were polished with 600-grit SiC polishing paper. The polished membrane was then sealed to the end of an Al_2O_3 tube by means of an assembly described elsewhere [1, 2]. During the measurements, nitrogen was bubbled through a water bath at a fixed temperature, and then was flowed over one side of the membrane, defined as the hydrogen-production side. The water's temperature was adjusted to control the water partial pressure (pH_2O) on the hydrogen-production side of the membrane. A gas of 4-80% H_2/balance helium was flowed over the other side of the membrane, called the oxygen-permeate side. Hydrogen on the oxygen-permeate side reacts with oxygen diffusing through the OTM, thus fixing a low pO_2 on the oxygen-permeate side

and establishing a pO_2 gradient across the OTM. Using hydrogen to produce hydrogen is impractical, of course, but it demonstrates that significant quantities of hydrogen can be produced if a large pO_2 gradient is established across the OTM. Hydrogen-helium mixtures were prepared by mixing ultrahigh-purity (UHP) hydrogen and UHP helium with mass flow controllers. A Hewlett-Packard 6890 gas chromatograph (GC) was used to measure hydrogen concentrations in the gas stream at temperatures of 500-900°C.

Figure 1 plots the hydrogen production rate versus inverse thickness for two types of CGO/Ni membrane that were made from CGO/NiO powder. One type of membrane was coated with porous layers, and one was not. Data in Fig. 1 were also obtained for two types of membrane made from mechanically mixed CGO/Ni powder, one with porous layers and one without. For thick membranes (i.e., inverse thickness < ≈2 mm^{-1}), the hydrogen production rate is not strongly influenced by the type of membrane and shows a roughly linear dependence on the inverse thickness. In this thickness regime, oxygen removal and hydrogen production are limited by bulk diffusion. By contrast, the hydrogen production rate for thin membranes (inverse thickness > 4 mm^{-1}) varied significantly with the type of membrane. Both porous layers and starting powder (CGO/NiO vs. CGO/Ni) influenced the hydrogen production rate of thin membranes.

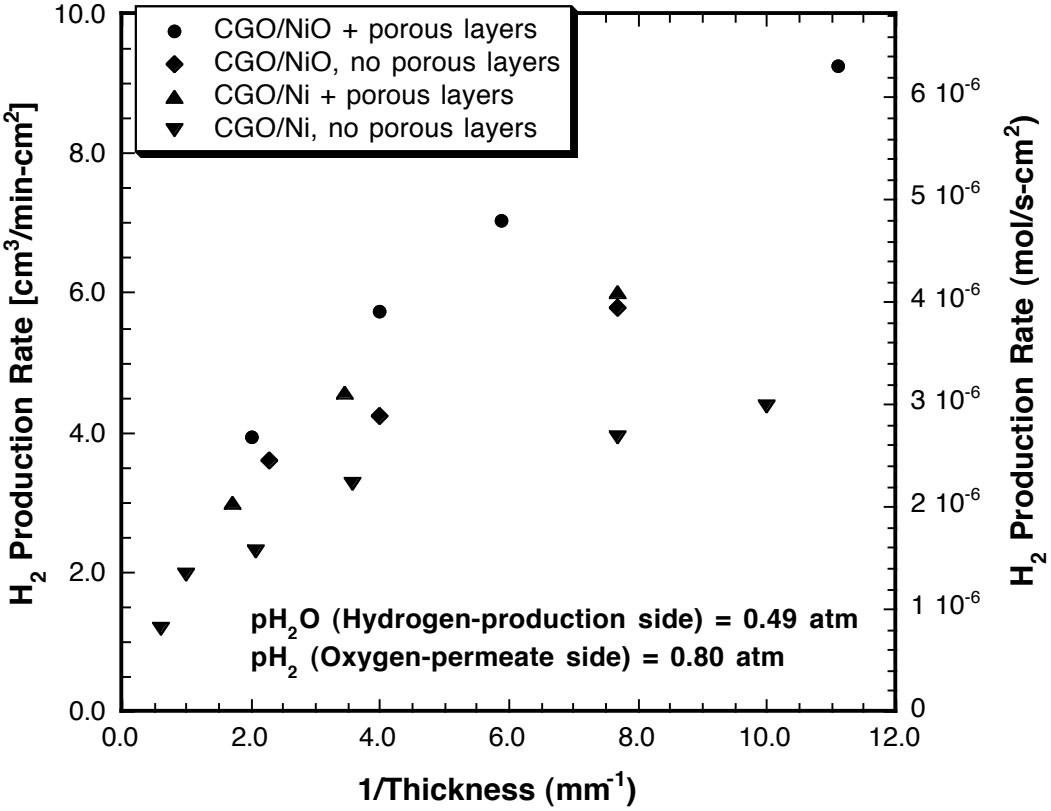

Fig. 1 Hydrogen production rate at 900°C for CGO/Ni membranes made by reducing CGO/NiO powder and sintering at 1150°C (with and without porous surface layers) or by mechanically mixing CGO/Ni powder and sintering at 1400°C (with and without porous surface layers).

The data in Fig. 1 indicate that porous surface layers significantly increased the hydrogen production rate of thin membranes made with either CGO/NiO or mechanically mixed CGO/Ni powder. The effect of porous layers was shown previously for membranes made with mechanically mixed CGO/Ni powder. Porous layers enhance the reaction kinetics on the surface by extending the triple-phase boundary (i.e., the region where ionic conductor, electronic conductor, and gas phase meet) beyond the membrane's dense interior. This condition increases the triple-phase-boundary area and enhances the dissociation and recombination of oxygen. Porous layers do not, however, affect the hydrogen production rate for thick membranes (inverse thickness <2 mm^{-1}), whose properties are limited by bulk diffusion.

Figure 1 also indicates that the hydrogen production rate is higher for membranes made with CGO/NiO powder sintered at 1150°C than for membranes made with CGO/Ni powder sintered at 1400°C, indepenent of whether the membranes have porous layers or not. Figure 2 shows micrographs for the two types of CGO/Ni membrane. The light-shaded ceramic and dark-shaded metal phases are clearly finer and more intimately mixed in the membrane made from CGO/NiO powder (Fig. 2b). As a result of their finer microstructure, membranes made from CGO/NiO powder have a larger triple-phase boundary area, which enhances the surface reaction kinetics and increases the hydrogen production rate. A maximum hydrogen production rate of ≈6 cm^3 (STP)/min-cm^2 was reported previously for a membrane with porous layers that was made from CGO/Ni powder. The maximum rate for a membrane made from CGO/NiO powder with porous layers was increased to ≈10 cm^3 (STP)/min-cm^2.

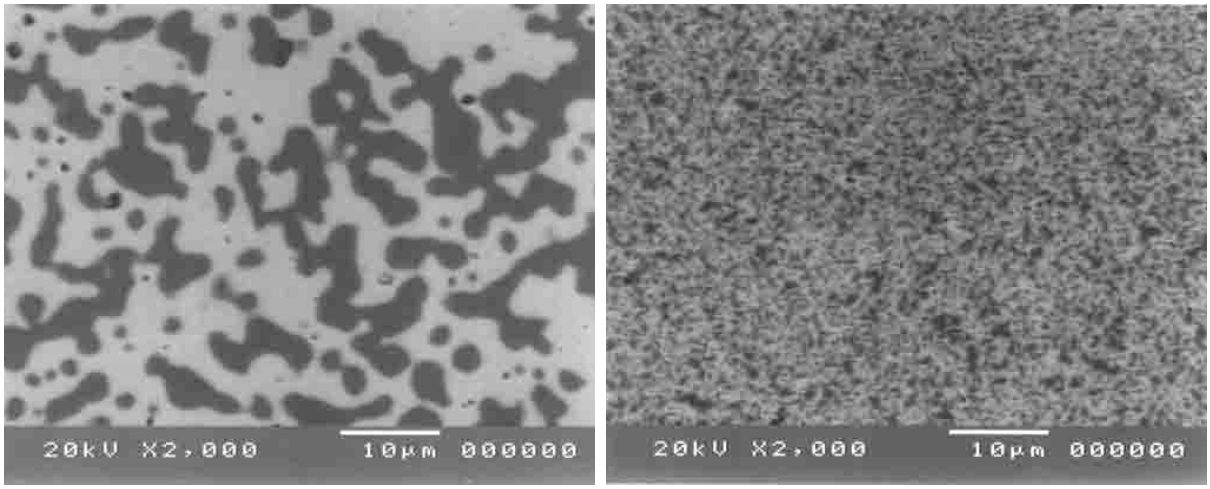

(a) (b)

Fig. 2 Backscattered electron micrographs for membranes made from a) CGO/Ni powder sintered at 1400°C and b) CGO/NiO powder sintered at 1150°C. Dark areas show Ni; light areas, CGO.

B) $SrFeCo_{0.5}O_x$ (SFC2) Membranes

SFC2 is a mixed oxygen ion-electron conductor that we developed earlier [9, 10] to separate oxygen from air for producing syngas (a mixture of carbon monoxide and hydrogen) from methane. It yields significantly higher hydrogen production rates than CGO/Ni membranes at high temperatures (≥850°C). To obtain the initial hydrogen production rate, SFC2 powder from Praxair was uniaxially pressed into pellets that were sintered in 200 ppm H_2/balance N_2 for 10 h at 1200°C.

Figure 3 plots the hydrogen production rate versus ΔpO_2 for SFC2 and CGO/Ni membranes. The term ΔpO_2 is defined here as pO_2(high)/pO_2(low), where pO_2(high) is the pO_2 on the hydrogen-production side, and pO_2(low) is the pO_2 on the oxygen-permeate side. The data are plotted versus ΔpO_2 to emphasize that the oxygen partial pressure difference across the membrane drives the production of hydrogen. A gas of N_2/0.49 atm H_2O flowed on the hydrogen-production side during these measurements, while ΔpO_2 was varied by changing pH_2 on the oxygen-permeate side. The pO_2(high) was calculated from the equilibrium constant for water dissociation using pH_2 and pH_2O on the hydrogen-production side, where pH_2 was measured by the GC, and pH_2O was calculated from the water bath's temperature (corrected for the H_2O that dissociated). Likewise, pO_2(low) was calculated from pH_2 and pH_2O on the oxygen-permeate side, where pH_2 was fixed by the H_2/He gas mixture (corrected for H_2 that reacted with oxygen emerging from the OTM), and pH_2O was equivalent to the pH_2 produced on the hydrogen-production side.

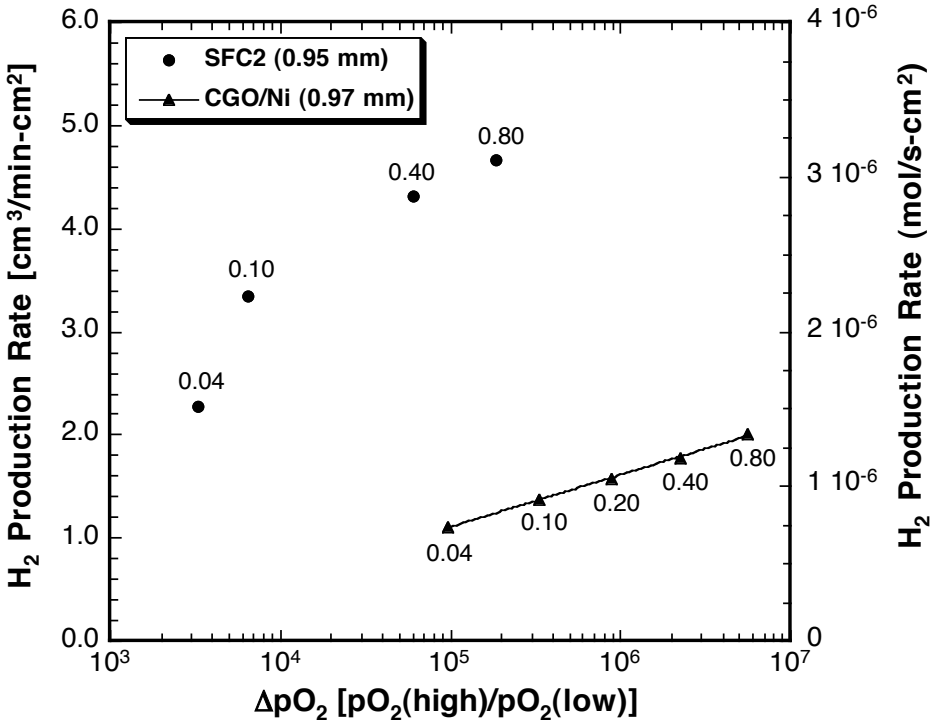

Fig. 3 Hydrogen production rate at 900°C for SFC2 and CGO/Ni versus oxygen partial pressure gradient. Numbers in figure give pH_2(atm) for gas on oxygen-permeate side. Inset gives membrane thickness.

Figure 3 compares the hydrogen production rates of thick (≈1 mm) SFC2 and CGO/Ni membranes. The difference in membrane thickness was much too small to explain the large difference in hydrogen production rate for the two membranes. For the membrane made from CGO/Ni powder, the powder source is not important at this thickness (Fig. 1) because the properties are limited by bulk diffusion. At a given ΔpO_2, the hydrogen production rate is much higher for SFC2 than for CGO/Ni, indicating that the oxygen flux through SFC2 is much higher. At a given pH_2 on the oxygen-permeate side, ΔpO_2 is much smaller for SFC2 than for CGO/Ni, because the high oxygen flux through SFC2 reduces the difference in pO_2 across the membrane. For example, when $pH_2 = 0.04$ atm on the oxygen-permeate side, ΔpO_2 is on the order of 10^5 for the CGO/Ni membrane, but is only ≈3000 for the SFC2 membrane. The curvature in the plot of hydrogen production rate versus ΔpO_2 for SFC2 suggests that surface kinetics might limit the hydrogen production rate, even at this high membrane thickness. If the rate is limited by surface reaction kinetics, applying porous surface layers to SFC2 membranes might enhance their hydrogen production rate.

To clarify whether the hydrogen production rate for SFC2 is limited by bulk diffusion or surface kinetics, we measured the rate as a function of membrane thickness (0.21-1.76 mm). The hydrogen production rate of SFC2 was measured with $pH_2O = 0.49$ atm on the hydrogen-generation side and $pH_2 = 0.8$ atm on the oxygen-permeate side. Figure 4 shows the results of these measurements. Lines in the figure are shown only to facilitate discussion.

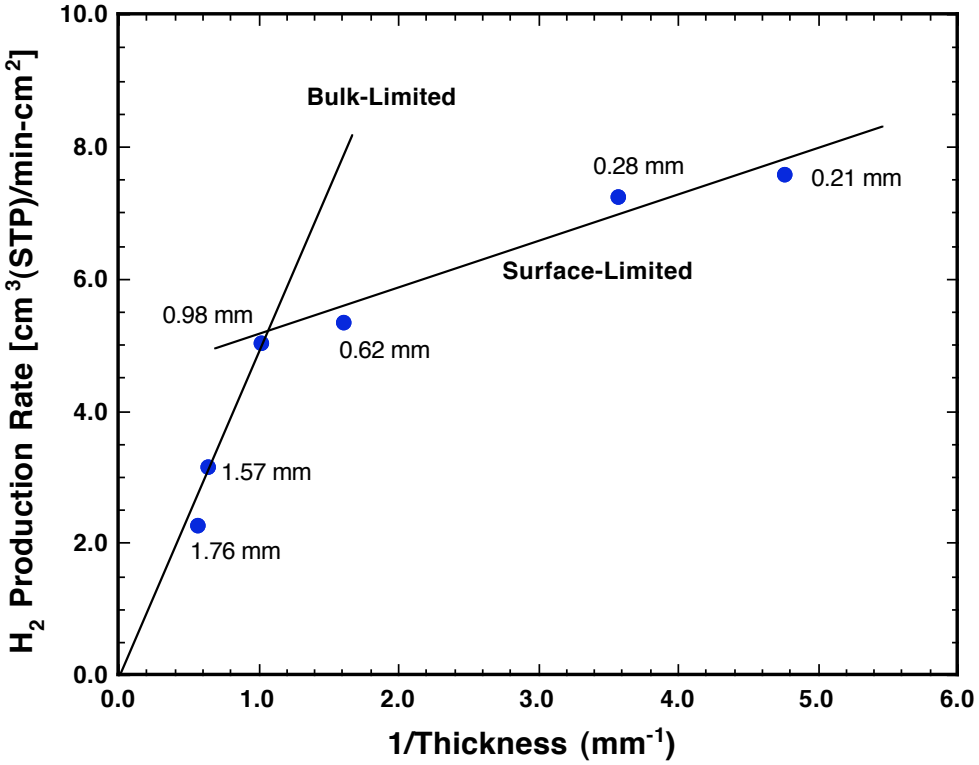

Fig. 4 Hydrogen production rate at 900°C for uniaxially pressed SFC2 disks with pH_2O=0.49 atm on hydrogen-generation side and pH_2=0.8 atm on oxygen-permeate side. Numbers in figure give membrane thickness.

For thick (≥0.98 mm) membranes, the hydrogen production rate (Fig. 4) varies linearly with the inverse of membrane thickness and extrapolates to zero, indicating that bulk diffusion limits hydrogen production in this thickness regime. The hydrogen production rate also varies linearly with the inverse of membrane thickness over the range 0.21-0.98 mm, but it does not extrapolate to zero. The rate increases from 5.0 $cm^3/min\text{-}cm^2$ for a 0.98-mm-thick membrane to 7.6 $cm^3/min\text{-}cm^2$ for a 0.21-mm-thick membrane. The hydrogen production rate for the 0.21-mm-thick membrane is only ≈50% larger than that for the 0.98-mm-thick membrane, but it should be about five times larger if hydrogen production is limited by the diffusion of oxygen through the membrane's bulk. This discrepancy and the fact that the data for this thickness range do not extrapolate to the origin indicate that surface reaction kinetics limit the hydrogen production of thin membranes. Coating thin membranes with porous layers should enhance the surface reaction kinetics and yield considerably higher hydrogen production rates.

To increase the hydrogen production rate of SFC2 membranes, both surfaces of thin (0.25-0.50 mm) membranes made by uniaxial pressing were coated with porous SFC2 layers. Figure 5 compares the hydrogen production rates of surface-modified and unmodified SFC2 membranes at 900°C; these rates were measured with wet N_2 (pH_2O = 0.49 atm) on the hydrogen-generation side and dry H_2 (pH_2 = 0.8 atm) on the oxygen-permeate side.

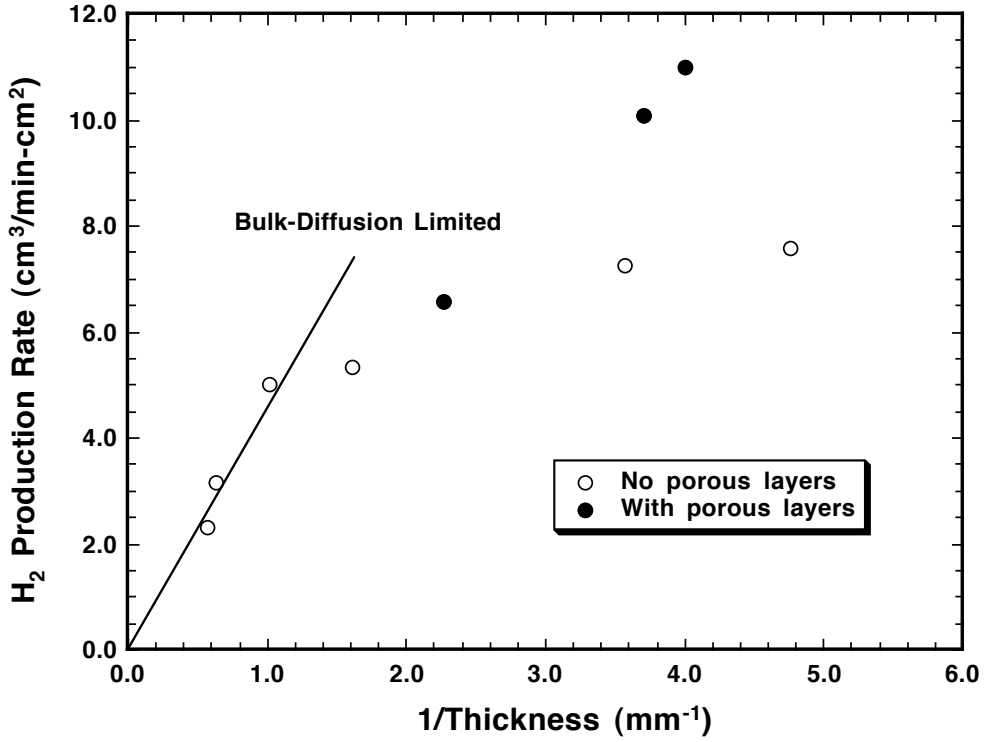

Fig. 5 Hydrogen production rate vs. inverse of thickness for SFC2 membranes with and without porous SFC2 layers. Line indicating bulk diffusion-limited regime is drawn merely as an aid to the eye.

Porous SFC2 layers increased the surface area of coated membranes and enhanced their hydrogen production rate relative to unmodified membranes. As seen in Fig. 5, a membrane with thickness of ≈0.25 mm gave a rate of ≈11 $cm^3/min\text{-}cm^2$. The effect of porous layers becomes more pronounced as the membrane thickness decreases, because the effect of surface oxygen exchange kinetics becomes more dominant. A similar effect was also observed in our previous studies with Ni/CGO cermet membranes. The data for membranes with porous layers do not fall on the extrapolated line for samples limited by bulk diffusion, suggesting that the microstructure of the porous layers has not been optimized. As a result, the porous layers enhance the hydrogen production rate but do not entirely eliminate the limitations from surface reaction kinetics.

Figure 5 indicates that decreasing the membrane thickness can further increase the hydrogen production rate if limitations from surface reaction kinetics are overcome by coating the membranes with porous layers. To prepare thinner membranes with sufficient mechanical integrity for routine handling, we began developing methods to fabricate SFC2 films on catalytically active porous substrates. Figure 6 shows a scanning electron micrograph from a fracture surface of an ≈40-μm-thick SFC2 film on a porous Ni/CGO substrate. To improve adhesion between the film and substrate, the NiO/CGO substrate was first coated with a thin "bond" layer of NiO/SFC2 and then was coated with a colloidal dispersion of SFC2. The twice-coated disk was sintered in 200 ppm H_2/balance N_2 for 9 h at 1250°C, then cooled to 850°C, after which the gas was switched to 4% H_2/balance N_2. To reduce NiO and create porosity in the substrate, the sample was held at 850°C for 2 h before it was cooled to room temperature.

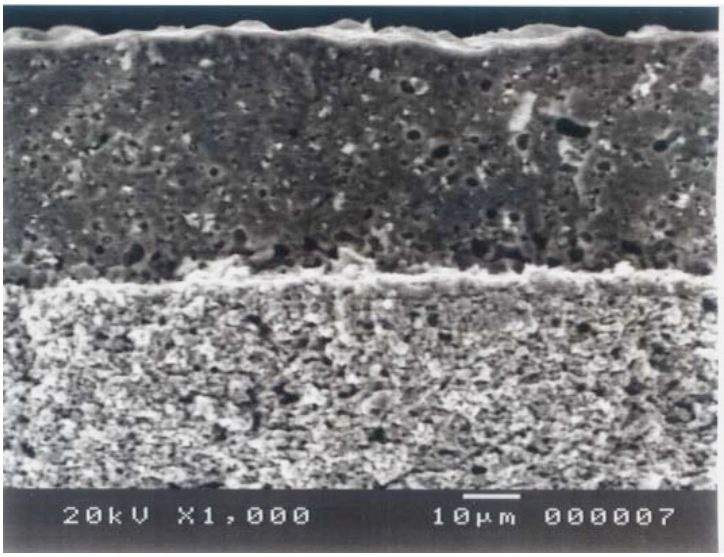

Fig. 6. Secondary electron image from fracture surface of SFC2 film on Ni/CGO substrate after sintering.

Figure 7 shows the hydrogen production rate versus pH_2O on the hydrogen-generation side of an ≈0.05-mm-thick SFC2 film on a Ni/CGO substrate. As expected, the hydrogen production rate increased with increasing pH_2O but reached only 5.4 $cm^3/min\text{-}cm^2$ with pH_2O ≈0.5 atm. We expected a significantly higher rate based on Fig. 4, which shows a hydrogen production rate of 7.6 $cm^3/min\text{-}cm^2$ for a thicker (0.21 mm) SFC2 disk without a porous surface layer. This low hydrogen production rate might have resulted from a reaction between SFC2 and NiO in the bond layer. The bond layer might also have restricted oxygen permeation due to its lower volume fraction of SFC2.

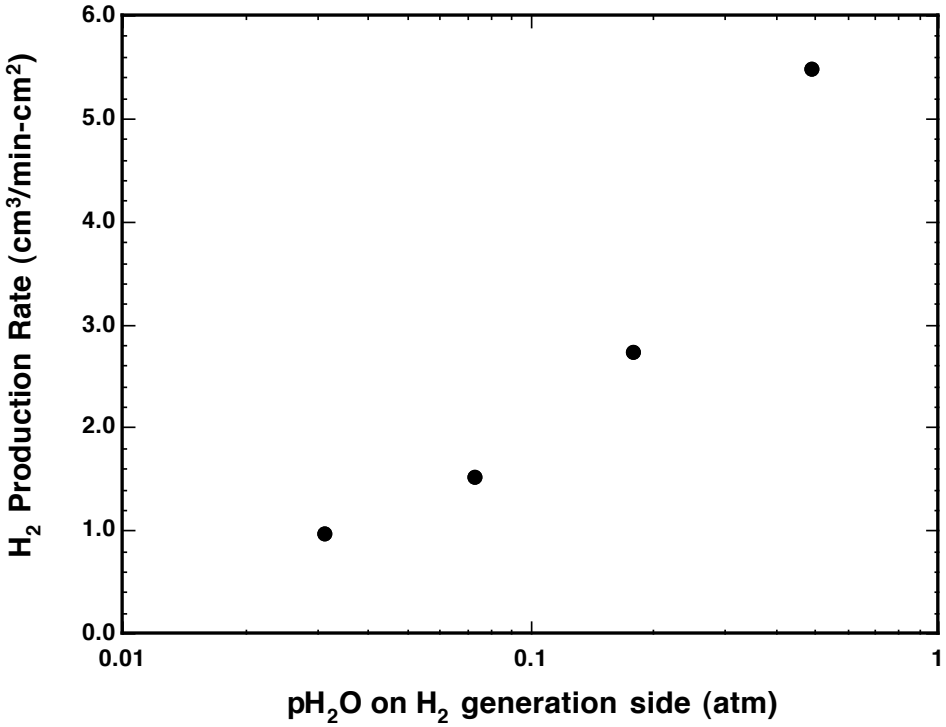

Fig. 7. Hydrogen production rate vs. pH_2O on hydrogen-generation side of SFC2 thin film at 900°C using 80% H_2/balance He on oxygen-permeate side.

To prevent reactions between SFC2 and its substrate, SFC2 thin films were fabricated on porous SFC2 substrates. Porous SFC2 substrates were prepared by blending a homogeneous mixture of SFC2 (Praxair Specialty Ceramics) and carbon (Fisher Scientific, 20-30 wt.%) powders with a binder. The mixture of SFC2, carbon, and binder was milled in isopropyl alcohol for 24 h, then the alcohol was evaporated, and the dried powder was sieved with a 120-mesh screen. The powder was uniaxially pressed (200 MPa) into thin (≈2 mm) cylindrical disks (22-mm dia.) that were pre-sintered at 950-1000°C for 5 h in air to remove the carbon and provide the disks with some mechanical integrity.

Thin-film membranes of SFC2 were fabricated from a colloidal suspension that contained SFC2 powder with an average particle size of ≈0.9 μm. The SFC2 powder and an organic dispersant were mixed in isopropyl alcohol for 30 min in an ultrasonic bath to break up agglomerates and disperse the powders. To deposit a thin film, the colloidal suspension

was cast onto a partially sintered SFC2 substrate. The green film and substrate were then sintered in either ambient air or ≈200 ppm H_2/balance N_2. The hydrogen production rate of SFC2 films was measured by the procedures described above for testing CGO/Ni membranes.

A challenge in fabricating dense SFC2 films on porous SFC2 substrates is maintaining sufficient porosity in SFC2 substrates because they densify easily during sintering of the SFC2 film. To retain the porosity in the substrates, carbon powder was incorporated as a pore former in green substrates. Figure 8 shows the fracture surfaces of SFC2 substrates sintered at 1160 and 1210°C in 200 ppm H_2/N_2. Both substrates were prepared with a powder mixture that contained 30 wt.% carbon. After sintering at 1160°C, the porosity in the substrate appeared to be uniformly distributed and adequate for good gas transport (Fig. 8a), but the level of porosity was significantly reduced when the sintering temperature was raised only 50°C (Fig. 8b). Reducing the carbon content in the powder mixture to 20 wt.% (Fig. 9) also decreased the substrate's porosity, but probably not enough to seriously impede gas transport. Based on these results, SFC2 films were prepared on substrates made from SFC2/carbon mixtures with 20-30 wt.% carbon and were sintered at 1160°C.

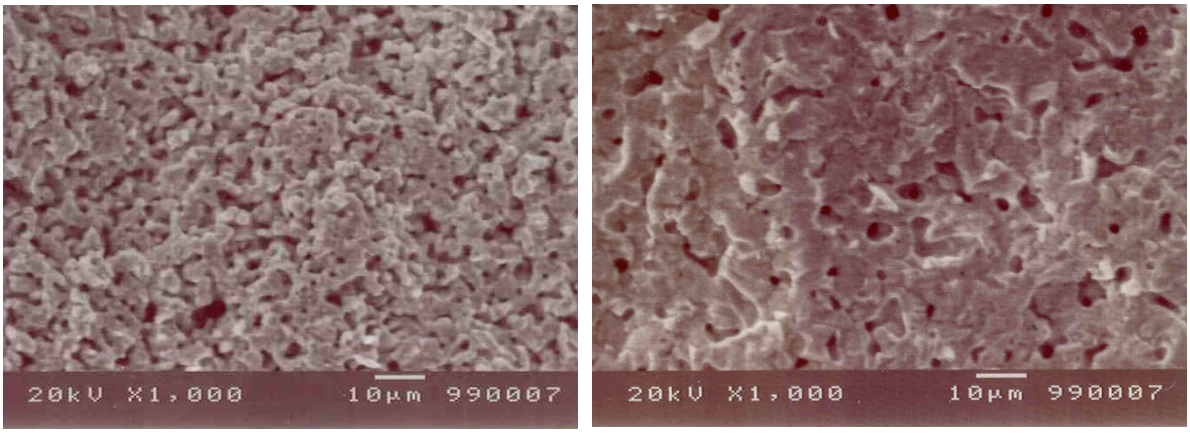

(a) (b)

Fig. 8 Fracture surface of SFC2 substrates sintered in 200 ppm H_2 for 10 h at a) 1160 and b) 1210°C. The SFC2 powder contained 30 wt.% of carbon.

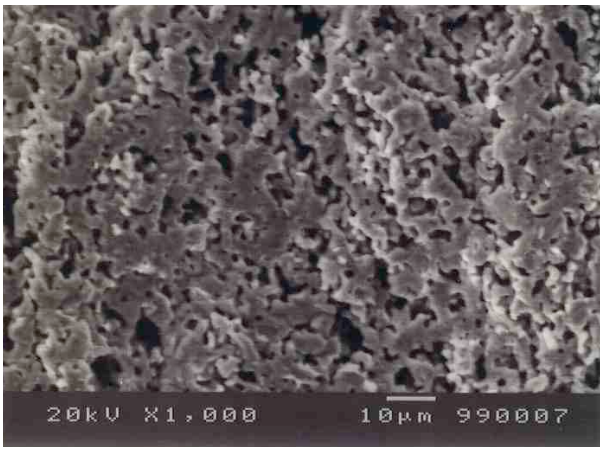

Fig. 9 Fracture surface of SFC2 substrate sintered in 200 ppm H_2 for 10 h at 1160°C. The SFC2 powder contained 20 wt.% of carbon.

The atmosphere during sintering significantly influences the properties of SFC2 thin films. The films were sintered in an atmosphere of either 200 ppm H_2/balance N_2 or ambient air. Figure 10 shows fracture surfaces of films made on substrates prepared from a powder mixture containing 20 wt.% carbon and sintered in 200 ppm H_2/balance N_2 at 1160°C for 7 h. The films contain only isolated porosity whereas the substrates have sufficient porosity. Varying the number of times that SFC2 was cast onto the substrate gave acceptable control of the film's thickness. One film had a thickness of ≈20 μm (Fig. 10a), and the other a thickness of ≈50 μm (Fig. 10b). Although the film's density and substrate's porosity are satisfactory, films sintered in 200 ppm H_2/balance N_2 tended to crack and/or warp during sintering.

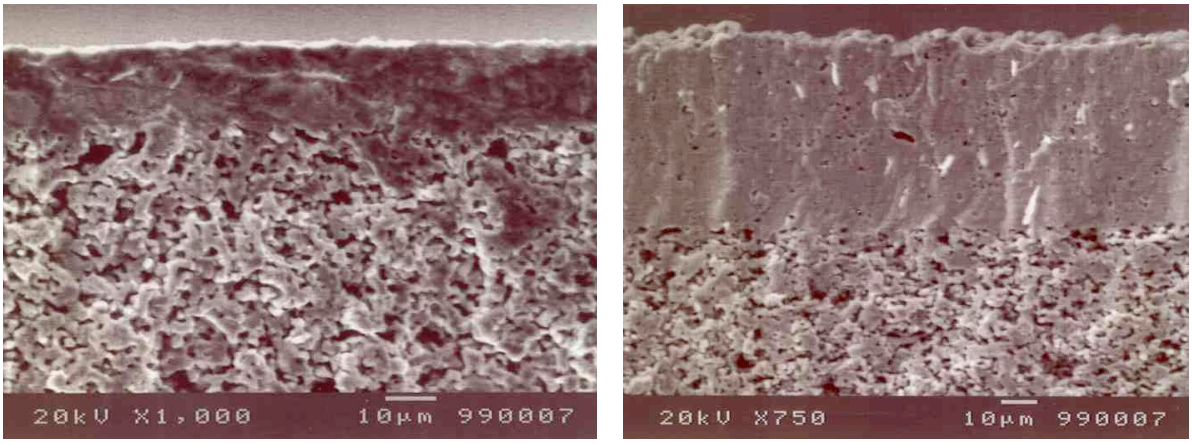

(a) (b)

Fig. 10 Fracture surface of as-sintered SFC2 films after coating substrate with SFC2 colloid (a) two and (b) three times.

In contrast to SFC2 films sintered in 200 ppm H_2/balance N_2, SFC2 films sintered in air were flat and free of cracks. To enhance surface reaction kinetics and increase the hydrogen production rate of air-sintered films, their top surface was coated with a layer of porous SFC2. The hydrogen production rate at 900°C was measured as a function of pH_2O on the hydrogen-generation side of the membrane, while dry 80% H_2/balance He was flowed on the oxygen-permeate side. Figure 11 compares the hydrogen production rates of a thin-film membrane (thickness ≈30 μm) sintered in air and a disk membrane (thickness ≈210 μm) sintered in 200 ppm H_2.

The hydrogen production rate is low for the thin-film membrane sintered in air, considering that the disk membrane was much thicker and had no porous layers whereas both surfaces of the thin film were coated with porous SFC2 layers (Fig. 12). A significantly higher hydrogen production rate was expected on the basis of earlier thickness-dependence measurements (Fig. 5). Because both the film and substrate contained only SFC2, it was unlikely that the low hydrogen production rate was caused by a chemical reaction between the film and substrate. Microscopy suggested that the low hydrogen production rate was related instead to the film's microstructure.

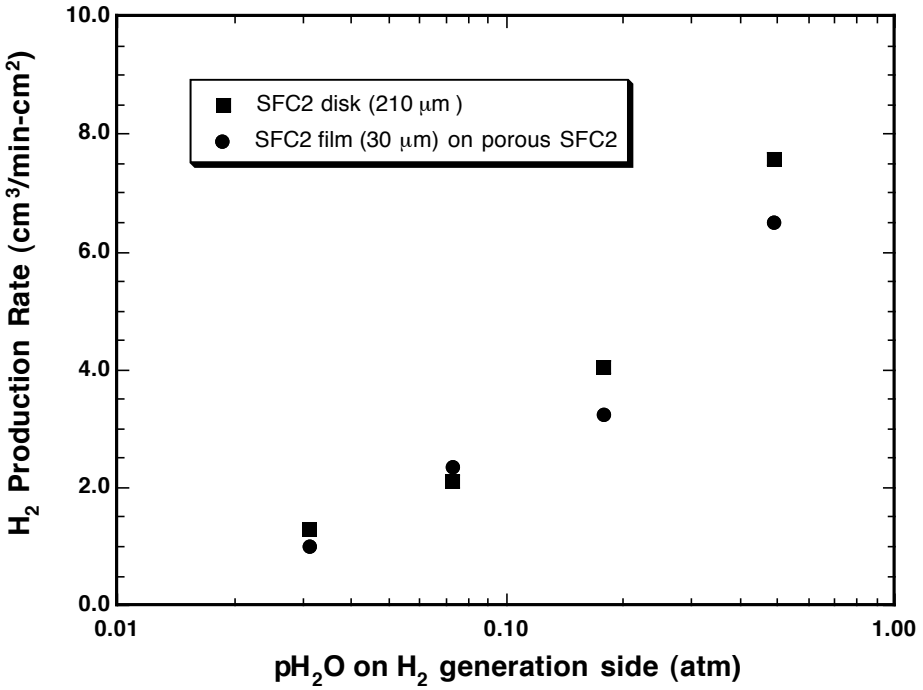

Fig. 11 Hydrogen production rate of SFC2 membranes at 900°C with dry 80% H_2/balance He on oxygen-permeate side. The thicknesses of the film and disc were 30 μm and 210 μm, respectively.

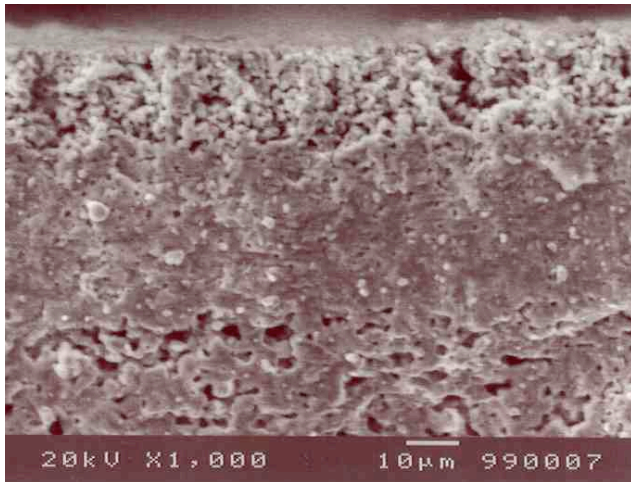

Fig. 12 Fracture surface of SFC2 film after testing.

As-sintered surfaces of SFC2 samples sintered in 200 ppm H_2 and in air are shown in Fig. 13. An SFC2 film sintered in ambient air (Fig. 13a) had big (>5 μm) plate-like crystals and gave a low hydrogen production rate. By contrast, a film sintered in 200 ppm H_2 had small (1-2 μm) equiaxed grains (Fig. 13b); uniaxially pressed SFC2 disks sintered in the same atmosphere have given a high hydrogen production rate. These results suggest that the finer, equiaxed microstructure is conducive to a high hydrogen production rate; consequently, we worked to develop procedures to sinter flat, crack-free thin films in a reducing environment.

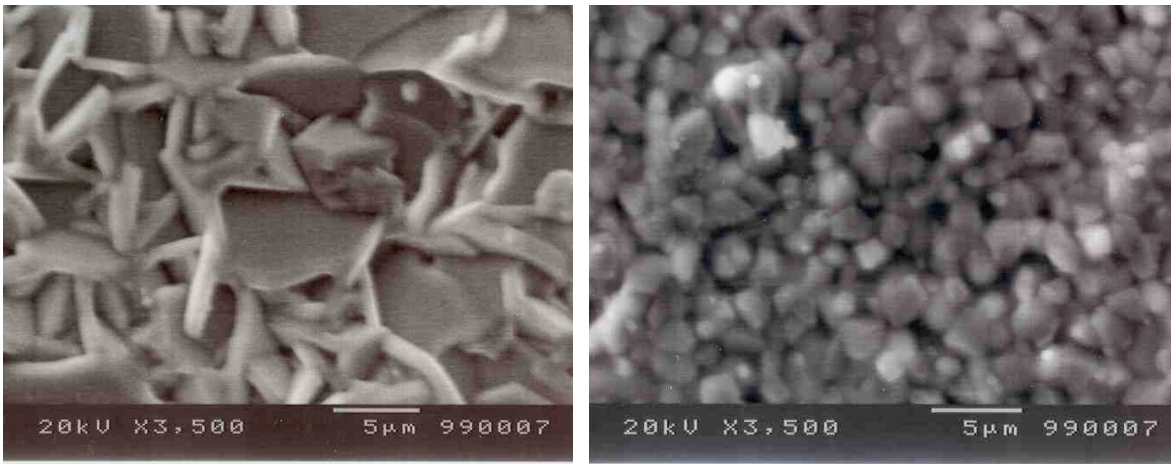

(a) (b)

Fig. 13 As-sintered surfaces of SFC2 films sintered in (a) air and (b) 200 ppm H_2.

Sintering SFC2 thin films in an atmosphere of argon and then annealing them at an intermediate temperature (750°C) enabled the fabrication of flat, crack-free films with a fine, equiaxed microstructure. Figure 14 shows scanning electron images of an SFC2 film that was sintered in Ar for 7 h at 1160°C and then annealed for 5 h at 750°C. Substrates for the films were prepared from a SFC2 powder mixture that contained 20 wt.% carbon. The film had a thickness of ≈20 µm (Fig. 14a). Figures 14b shows that SFC2 films sintered in Ar appear dense and have small equiaxed grains, as do films sintered in 200 ppm H_2 (Fig. 13b). Plate-like crystals are not evident after sintering in either of these atmospheres.

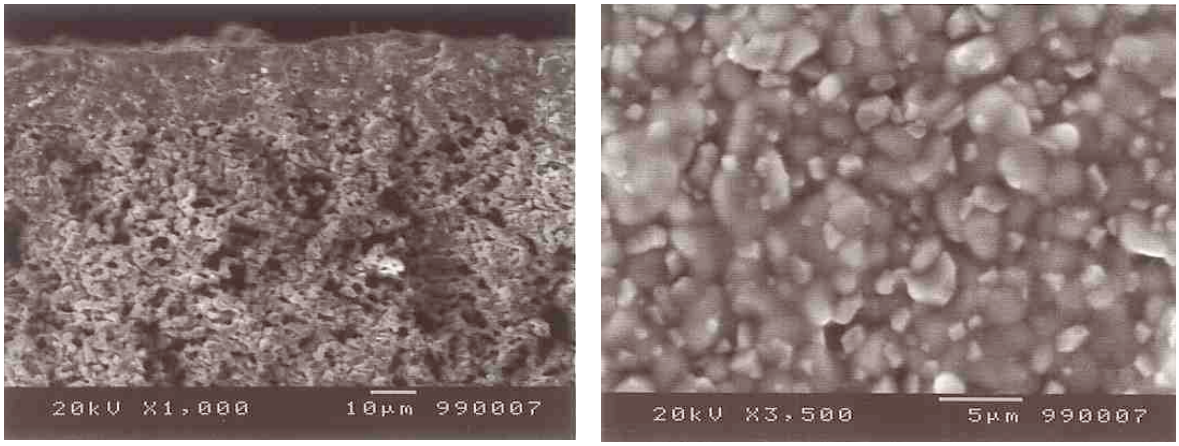

(a) (b)

Fig 14 Secondary electron images of SFC2 film sintered in Ar for 7 h at 1160°C and annealed for 5 h at 750°C: (a) fracture surface after hydrogen production rate measurements and (b) as-sintered surface. Substrates were prepared from SFC2 powder with 20 wt.% carbon

The sintering atmosphere significantly influenced the hydrogen production rate of SFC2 thin films, as suggested by earlier results (Fig. 11). The hydrogen production rate was measured at 900°C as a function of pH_2O on the hydrogen-generation side of membranes while flowing dry H_2 (pH_2=0.8 atm) on the oxygen-permeate side. Figure 15 compares the hydrogen production rate of two sets of SFC2 films sintered in air and two sets sintered in Ar. The rates for the Ar-sintered films are similar to those of air-sintered films at low pH_2O but are much higher at high pH_2O. With pH_2O=0.49 atm on the hydrogen-generation side, an argon-sintered film (thickness ≈20 μm) gave a hydrogen production rate of 12.4 $cm^3/min\text{-}cm^2$, which is the highest hydrogen production rate produced to date in tests using an Argonne OTM. The higher hydrogen production rate for Ar-sintered films is believed to result from the microstructure of the film.

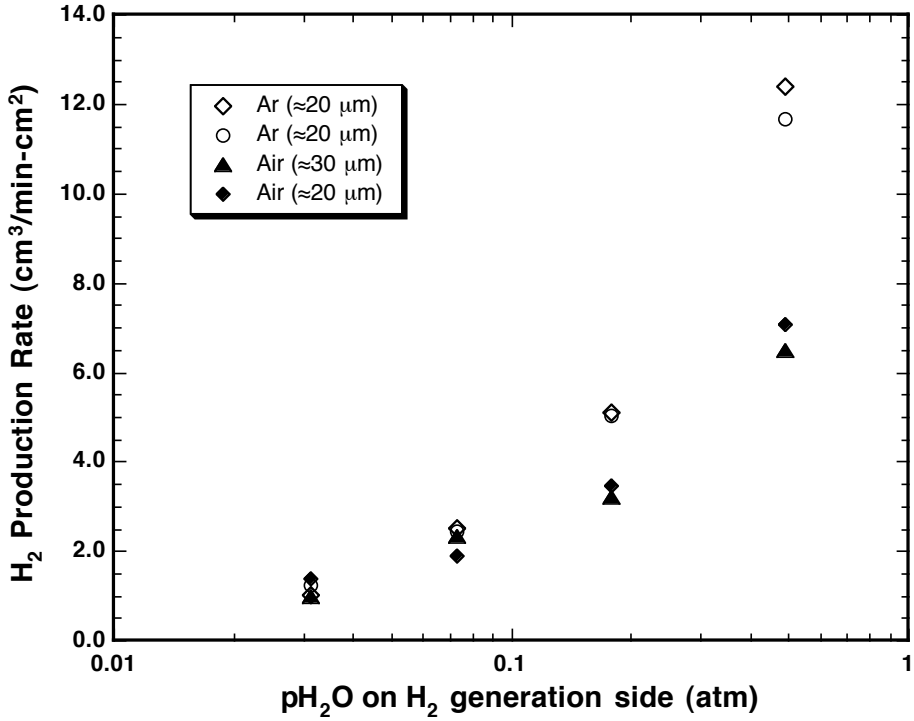

Fig. 15 Hydrogen production rate vs. pH_2O on hydrogen-generation side of SFC2 membranes at 900°C using 80% H_2/balance He on oxygen-permeate side.

C) Sr-Fe-Ti-Oxide (SFT) Membranes

Although SFC2 is a promising material for OTMs due to its high hydrogen production rate at high temperatures (>850°C), a phase transition dramatically reduces its hydrogen production rate at temperatures below ≈850°C. This is evident in Fig. 16, which compares the hydrogen production rates of SFC2 and CGO/Ni membranes. The hydrogen production rate for SFC2 is significantly higher at temperatures ≥850°C, but decreases dramatically at lower temperature due to the phase transition at 825-850°C. For this reason, SFC2 might be unsuitable for applications at low temperatures (<825°C). For applications at <850°C, we are investigating SFT membranes that do not undergo a phase transition like that of SFC2.

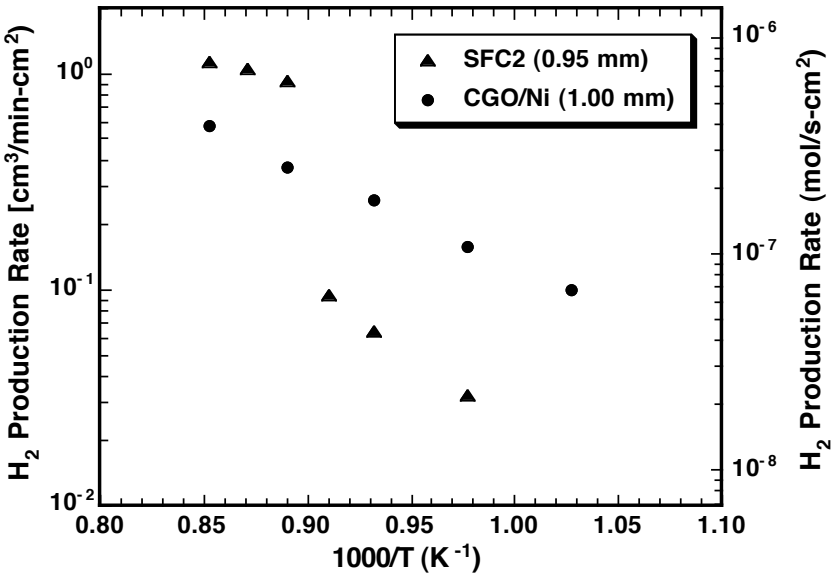

Fig. 16 Hydrogen production rate of SFC2 and CGO/Ni membranes with 4% H_2/He on oxygen-permeate side and pH_2O=0.03 atm on hydrogen-production side.

Figure 17 compares the hydrogen production rates of SFC2 and several SFT membranes with different compositions. The hydrogen production rate was measured with 4% H_2/He on the oxygen-permeate side of the membrane and wet N_2 (pH_2O=0.03 atm) on the hydrogen-production side. The hydrogen production rate for SFC2 is higher above 850°C but is much lower below 850°C due to its phase transition. Among SFT membranes tested, SFT2 gives the highest hydrogen production rate. To understand the effect of Ti doping on hydrogen production rate, detailed studies of the electrical conductivity of SFT membranes are needed.

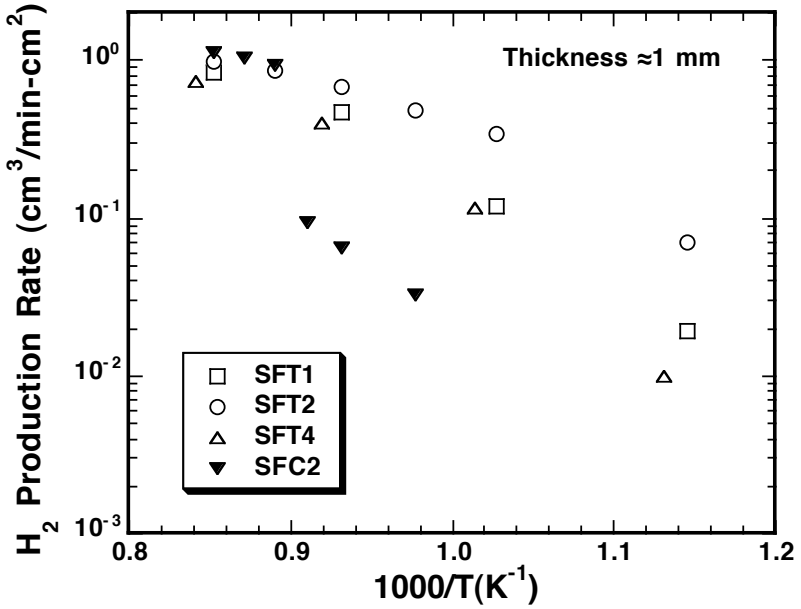

Fig. 17 Hydrogen production rate of SFT and SFC2 membranes with 4% H_2 He on oxygen-permeate side and pH_2O=0.03 atm on hydrogen-production side.

D) Tubular Membranes

To be practical, OTMs must be available in a shape that has a large active area, e.g., tubes; therefore, we began developing methods for fabricating tubular OTMs during FY 2007. In one method, OTM powder is loaded into a rubber mold (Trexler Rubber) with a stainless steel mandrel. It is then pressed in a cold isostatic press (Engineered Pressure Systems) at 10,000-15,000 psig. The tube is sintered after being removed from the mold and the mandrel. Figure 18 shows a photograph of SFC2 tubes after they were pressed and sintered for 10 h at 1150°C in argon. The tubes are now being tested with the spring-loaded fixture (Fig. 19) that we developed for measuring the hydrogen flux through HTMs.

Fig. 18 Sintered SFC2 tube prepared by cold isostatic pressing of SFC2 powder.

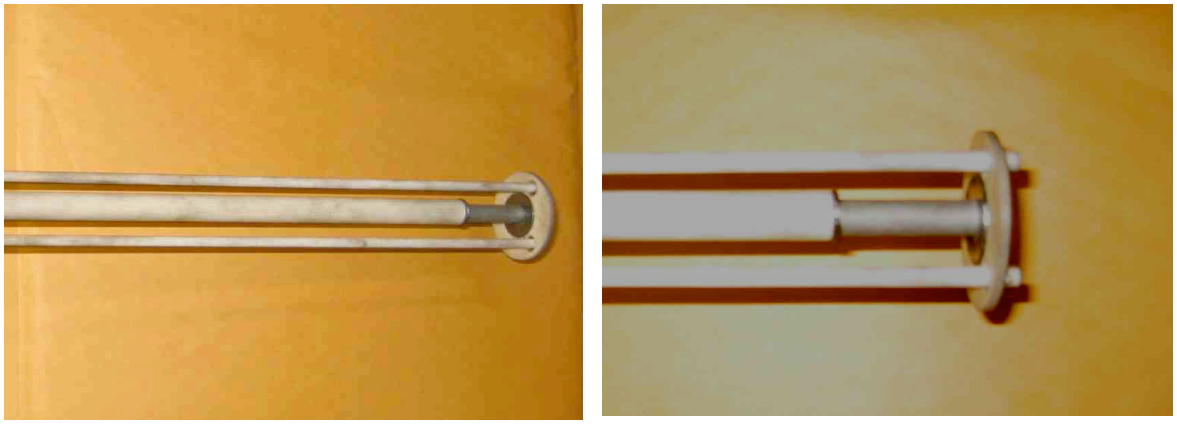

(a) (b)

Fig. 19 Spring-loaded fixture for measuring H_2 production rate of OTM tubes.

Figure 20 shows preliminary results from measuring the hydrogen production rate of one of the tubes shown in Fig. 18. The hydrogen production rate was measured at 900°C as a function of pH_2O on the hydrogen-generation side with dry H_2 (pH_2=0.8 atm) flowing on the oxygen-permeate side. Inlet flow rates of both N_2 and H_2 were fixed at 150 ml/min. The SFC2 tube had a length of 7.04 cm, an outside diameter of 1.26 cm, and a wall thickness of 0.07 cm. The surface area on the inside of the tube (23.4 cm^2) was used to normalize the hydrogen production rate (Fig. 20).

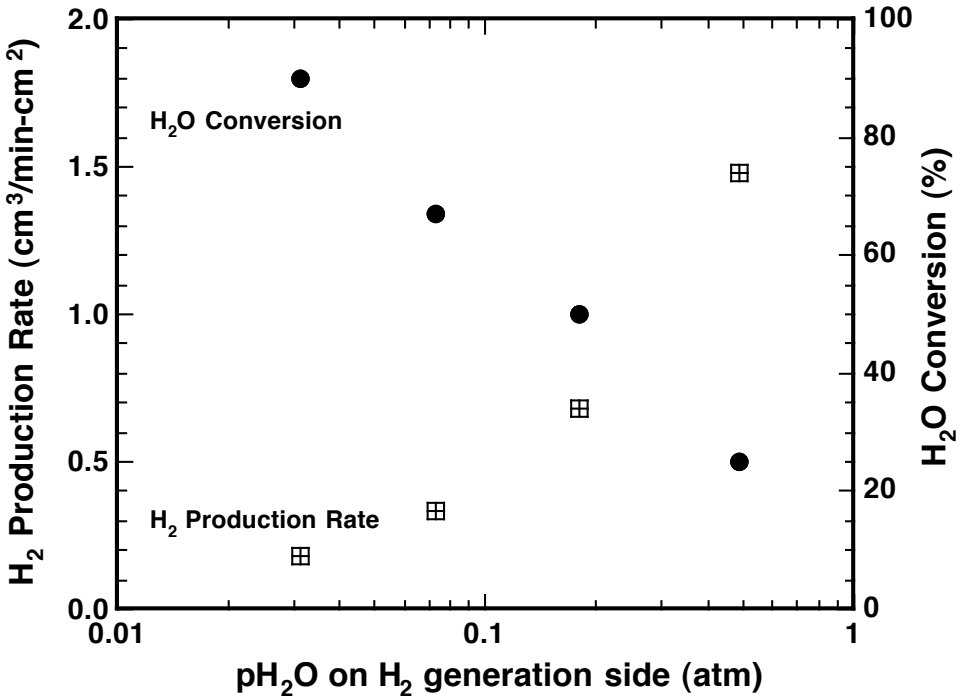

Fig. 20 Hydrogen production rate vs. pH_2O on hydrogen-generation side of SFC2 tube at 900°C using 80% H_2/He on oxygen-permeate side.

The hydrogen production rate for the SFC2 tube is about five times lower than that of a disk-type SFC2 membrane with similar thickness. The main cause for the low hydrogen production rate is believed to be concentration polarization on the hydrogen production side of the tube. Figure 20 shows a high conversion of steam (≈90% for pH_2O=0.03 atm and ≈25% for pH_2O=0.49 atm), which indicates that the flow rate of steam should be increased. In addition to depleting steam from the region near the tube's surface, the high conversion rate gives a high hydrogen concentration on the hydrogen-generation side (2.85% H_2 at pH_2O=0.03 atm and 19.2% at pH_2O=0.49 atm). The high hydrogen concentration lowers the oxygen partial pressure gradient across the membrane and decreases the hydrogen production rate. In the future, we will continue measuring the hydrogen production rate of the tube presently being tested and will begin fabricating OTM tubes with higher hydrogen production rates by the methods described above (i.e., coating with porous layers and reducing membrane thickness).

One method being developed to fabricate thin-walled OTM tubes is based on the paste-painting technique for fabricating HTM thin films. In this approach, we first produce porous alumina support tubes in a cold isostatic press by pressing alumina hydrate powder in a rubber mold with a stainless steel mandrel at 10,000-15,000 psig. After pressing, tubes are pre-sintered in air for 3-5 h at 800-950°C. Figure 21a shows a photograph of such a tube. After the tube is pre-sintered, a paste containing the OTM components is painted onto the tube's outside surface, and then the tube is sintered. Figure 21b shows a photograph of two porous alumina support tubes next to an HTM film that was sintered on a tubular porous alumina support. Typical tubes made by this method are 8-10 cm in length with an outside diameter of ≈1 cm and a membrane thickness of 25-50 μm.

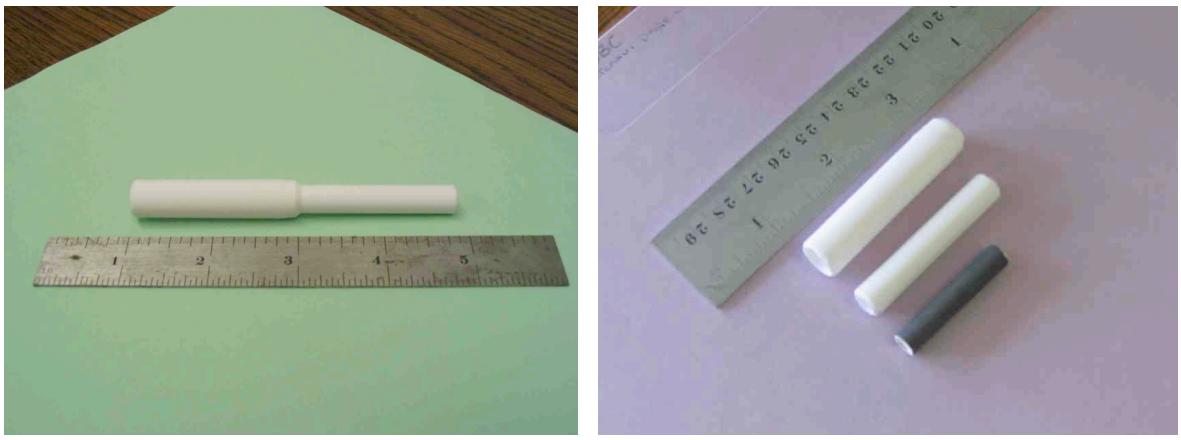

(a) (b)

Fig. 21 a) Porous alumina tube after pre-sintering for 5 h at 700-800°C in air and b) two porous alumina tubes and HTM film on porous alumina tube after sintering for 5 h at 1400°C in air.

V. FUTURE WORK

We will continue developing new materials to improve the performance of OTMs in producing hydrogen via coal/coal gas-assisted water splitting. This effort will involve both investigating entirely new membrane compositions and continuing to apply methods described in this report to enhance the hydrogen production rate of the OTMs we have already identified. Based on the principles of solid-state chemistry, we will prepare and test novel materials thought to have potential for high hydrogen production rates. To increase the hydrogen production rates of existing OTM materials, we will continue to improve methods for reproducibly fabricating membranes with thickness < ≈25 μm, and we will coat membranes with porous layers, working to optimize microstructural features of the porous layers, such as porosity and pore size. When the hydrogen production rate is significantly influenced by sintering conditions, we will optimize the sintering process to enhance hydrogen production.

We will fabricate tubular OTMs in FY2008 and measure their hydrogen production rate to begin demonstrating that OTMs are practical for large-scale industrial applications. Tubes are practical for large-scale industrial processes due to their large active area and the relative ease of their fabrication and gas-manifolding. Self-supporting SFC2 tubes were produced in FY2007, and the hydrogen production rate of one such tube was measured. The relatively thick (≈0.07 cm) walls of these tubes and their lack of porous surface layers limited their hydrogen production rate. We will try various methods to increase the hydrogen production rate of OTM tubes in FY2008, e.g., reducing the wall thickness of self-supporting tubes and fabricating thin-film OTM membranes on porous support tubes as described in this report. Whether the tubes are self-supporting or consist of thin films on porous supports, we will develop methods to coat both surfaces of the tubes with porous layers.

Oxygen transport membranes will be used in FY2008 to test a new concept of using coal combustion to drive water dissociation for hydrogen production. In this concept, coal is combusted on one side of an OTM, while water splitting produces hydrogen on the other side. The combustion of coal establishes the large gradient in oxygen chemical potential across the OTM that is necessary for a high hydrogen production rate, while the oxygen produced by water splitting is used for coal combustion. This process reduces the number of steps needed to produce hydrogen from coal, thereby increasing the process efficiency. The hydrogen produced is physically separated from carbon dioxide and all other impurities; therefore, hydrogen purification is simpler and more cost-effective. Gas separation costs are reduced because the OTM contains no precious metals. Because coal combustion is exothermic, the process supplies heat that is required for water splitting. In addition, the waste stream from the proposed process is ideal for sequestration, because it is rich in carbon dioxide.

Good chemical stability is a critical requirement for OTMs due to the high temperatures and corrosive environments they will encounter; therefore, we will begin evaluating the chemical stability of OTMs in FY2008. We will test the chemical and mechanical stability of OTMs in short-term (<100 h) exposures to industrially useful conditions, e.g., the atmospheres and temperatures that are typical for coal combustion and coal gasification. We will study the effect of syngas components on the hydrogen production rate of OTMs in the presence of H_2S and without H_2S. To assess the extent and course of reaction between the membrane and the atmosphere, the microstructure of membranes will be examined before and after exposures to industrial conditions.

We will evaluate process issues and economics as technical progress warrants. As directed by NETL's program managers, we will make contacts and hold discussions with potential collaborators. We will work with NETL's in-house R&D team and their Systems Engineering group to validate the process concept and assess the techno-economics of using OTMs to produce hydrogen by water splitting. We will provide technical input and engineering data to the NETL team to develop models for process viability and for thermal management studies.

VI. PUBLICATIONS, PATENTS, AND PRESENTATIONS

Hydrogen Production by High-Temperature Water Splitting Using Mixed Oxygen Ion-Electron Conducting Membranes, Proc. 201st Electrochem. Soc. Mtg., Philadelphia, PA, May 12-17, 2002.

Method for Generating Hydrogen by Catalytic Decomposition of Water, U.S. Patent 6,468,499, Oct. 22, 2002.

Hydrogen Production by Water Splitting Using Mixed Conducting Membranes, Proc. National Hydrogen Assoc. 14th Annual U.S. Hydrogen Meeting, Washington, DC, March 4-6, 2003.

Hydrogen Production by Water Dissociation Using Mixed-Conducting Membranes, presented at 225th Amer. Chem. Soc. Natl. Mtg., Fuel Chemistry Div., New Orleans, March 23-27, 2003.

Hydrogen Production by Water Dissociation Using Oxygen-Permeable Cermet Membranes, presented at 105th Ann. Mtg. of Amer. Ceram. Soc., Nashville, April 27-30, 2003.

Hydrogen Production by Water Dissociation Using Mixed Conducting Membranes, presented at Second Information Exchange Meeting on Nuclear Production of Hydrogen, Argonne Natl. Lab., Oct. 2-3, 2003.

Use of Mixed Conducting Membranes to Produce Hydrogen by Water Dissociation, Intl. J. of Hydrogen Energy, 29, 291-296 (2004).

Hydrogen Production from Water Splitting Using Mixed Oxygen Ion-Electron Conducting Membranes, U.S. Patent 6,726,893, Apr. 27, 2004.

Hydrogen Production by Water Dissociation Using Mixed-Conducting Ceramic Membranes, Proc. of National Hydrogen Association's 15th Annual U.S. Hydrogen Energy Conf., Los Angeles, CA, April 27-30, 2004.

Hydrogen Production from Water Using Mixed-Conducting Ceramic Membranes, presented at 15th World Hydrogen Energy Conf., Yokohama, Japan, June 27-July 2, 2004.

Development of Dense Ceramic Membranes for Hydrogen Production and Separation, presented at American Soc. for Materials--Annual Materials Solution Conf., Columbus, OH, Oct. 18-21, 2004.

Hydrogen Production by Water Splitting Using Dense Thin-Film Cermet Membranes, presented at Fall Meeting of Materials Research Society, Boston, Nov. 28-Dec. 2, 2005.

Hydrogen Production by Water Dissociation Using Mixed Oxygen Ion-Electron Conducting Membranes, presented at Electrochem. Soc. 2005 Fall Mtg., Los Angeles, Oct. 16-21, 2005.

Hydrogen Production by Water Dissociation Using Mixed-Conducting Dense Ceramic Membranes, invited presentation at Amer. Chem. Soc. 231st Natl. Mtg., Atlanta, March 26-30, 2006.

Hydrogen Production by High-Temperature Water Splitting Using Electron-Conducting Membranes, U.S. Patent 7,087,211, Aug. 8, 2006.

Mixed-Conducting Membranes for Hydrogen Production and Separation, presented at 2006 MRS Fall Meeting, Boston, MA, Nov. 27 - Dec 1, 2006.

Hydrogen Production by Water Dissociation Using Mixed-Conducting Dense Ceramic Membranes, Intl. J. of Hydrogen Energy, 32, 451 (2007).

Reforming of Natural Gas via Water Splitting Using Dense Ceramic Membranes, presented at Natl. Hydrogen Assoc. Meeting, San Antonio, TX, March 19-22, 2007.

Hydrogen Production by Water Splitting Using Mixed Ionic-Electronic Conducting Membranes, presented at 211th Meeting of Electrochem. Soc., Chicago, IL, May 6-10, 2007.

REFERENCES

[1] U. Balachandran et al., Argonne National Laboratory Hydrogen Separation Membranes--Annual Report for FY 2003.

[2] U. Balachandran et al., Argonne National Laboratory Hydrogen Separation Membranes--Annual Report for FY 2002.

[3] S. Ihara, Bull. Electrotech. Lab., 41, 259-280 (1977).

[4] B. Ma, et al., Ceram. Trans., 73, 169-177 (1997).

[5] P. S. Maiya, et al., Solid State Ionics, 99, 1-7 (1997).

[6] L. Qiu, et al., Solid State Ionics, 76, 321-329 (1995).

[7] T. H. Lee, et al., Solid State Ionics, 100, 77-85 (1997).

[8] H. Naito and H. Arashi, Solid State Ionics, 79, 366-370 (1995).

[9] U. Balachandran et al. Applied Catalysis A: General, 133,19-29 (1995).

[10] U. Balachandran et al. U. S. Patent 5,580,497 (1996).

Energy Systems Division
Argonne National Laboratory
9700 South Cass Avenue, Bldg. 212
Argonne, IL 60439-4838

www.anl.gov

A U.S. Department of Energy laboratory
managed by UChicago Argonne, LLC